PCCP

ROYAL SOCIETY OF CHEMISTRY

PAPER

View Article Online
View Journal



Cite this: DOI: 10.1039/d6cp00590j

# Ground and low-lying electronic states of the diatomic molecule TiV from quantitative multireference *ab initio* calculations

Magdalene Liosi and Aristotle Papakondylis *

Received 17th February 2026,
Accepted 2nd May 2026

DOI: 10.1039/d6cp00590j

rsc.li/pccp

The lowest electronic states of the transition intermetallic TiV molecule have been studied by first principles employing the multireference configuration interaction technique and large correlation consistent basis sets. The ground state was found to be of $X^4\Sigma^-$ symmetry with a binding energy of $D_0^0$ = 41.1 kcal mol$^{-1}$ and $r_e$ = 1.910 Å. Full potential energy curves were constructed for a total of 45 low-lying Λ–S states of TiV, extracting spectroscopic constants, as well. In addition, an effort was made to rationalize the nature of the chemical bond in the different states of the system.



## 1. Introduction

Titanium and vanadium, two of the early first-row transition elements, are known for forming very useful alloys with significant technological applications in fields ranging from aerospace engineering and tools to bioimplants. They are, also, highly involved in organometallic chemistry and heterogeneous catalysis. However, the "simple" intermetallic TiV diatomic species has been poorly investigated so far. Certainly, technical difficulties, both experimental and theoretical, make it rather hard to study this system in depth. TiV was first observed in cryogenic argon matrices at 4 K, in 1984 by Van Zee and Weltner Jr.[1] These workers studied the ESR spectrum of $^{47}Ti^{51}V$ and established that its ground state is of $^4\Sigma$ symmetry. Based on the observed hyperfine parameters, they proposed a $s\sigma^2d\sigma^1d\pi^4d\delta^2$ electron configuration with multiple bonding involving sσ and dσ bonds. At that time an estimate of 43.7 kcal mol$^{-1}$ for the Ti–V binding energy had been published by Miedema.[2] In 1985 Walsch and Bauschlicher[3] using the MCSCF method presented small portions of potential energy curves for three electronic states of $^4\Sigma^-$, $^2\Delta$, and $^4\Pi$ symmetries. The energetically lowest state was found to be $^4\Sigma^-$ consistent with the experimental observation of Van Zee and Weltner Jr.[1] For this state they calculated a TiV bondlength of 1.86 Å and a binding energy $D_e$ = 0.80 eV with respect to the excited Ti($^5$F;3d$^3$4s$^1$) + V($^6$D;3d$^4$4s$^1$) separated atoms. Seven years later, in 1992, Spain and Morse[4] used resonant two-photon ionization (R2PI) spectroscopy and determined an experimental value $D_0^0$ = 2.068 eV. In the same year Mattar and Hamilton[5] performed LSD-LCAO calculations on the $^4\Sigma^-$ state of TiV and reported $r_e$ = 1.77 Å and a binding energy $D_e^0$ = 5.88 eV relative to the ground state Ti($^3$F) + V($^4$F) asymptote. Gutzev *et al.*[6] in a 2004 paper titled "Periodic Table of 3d-metal dimers" presented DFT/BPW91 results on the ground state of TiV. They found for the $X^4\Sigma^-$ state: $r_e$ = 1.78 Å, $\omega_e$ = 562 cm$^{-1}$, and $D_0^0$ = 2.78 eV. They also claimed that the lowest excited state is of $^2\Gamma$ symmetry lying 0.29 eV higher than the ground-state. Finally, in 2023, Jiang and Liu[7] using DFT with eight different exchange–correlation functionals and several basis sets, found for the TiV binding energy very different values ranging from 0.70 to 1.90 eV depending on the functional/basis they used. To the best of our knowledge, these are all the experimental or theoretical data in the literature on the TiV dimer to date.

We undertook the present work with the aim of producing a comprehensive mapping and characterization of numerous low-lying bound electronic states of the TiV species. This is the only reliable way to assign the ground state and predict the correct ordering of the excited states of the system. It is well known that the interaction between two transition metals can give rise to a veritable zoo of hundreds of molecular states with different spatial and spin symmetries that are very closely spaced. This is a consequence of the existence of many asymptotic atomic channels very close to each other within a narrow energy interval of a few eV.

The Ti($^3$F) and V($^4$F) atomic ground states both have a $3d^{n-2}4s^2$ valence electron distribution, where $n$ is the number of valence electrons. The much larger spatial extent of the doubly occupied 4s orbitals, as compared to the 3d orbitals, prevents the shielded 3d electrons from interacting effectively in covalent bonding. As a result, the interaction of the two ground state atoms is only expected to be of the van der Waals (vdW) type. Bonding should therefore involve excited states of one or both atoms with half-filled or empty 4s subshells. In a

*Department of Chemistry, Laboratory of Physical Chemistry, National and Kapodistrian University of Athens, Panepistimiopolis, Athens 157 71, Greece. E-mail: papakondylis@chem.uoa.gr; Tel: +302107274565*

recent paper on the ScV,[8] it was shown that the majority of its lowest bound states stem from the $Sc(^2D;3d^14s^2) + V(^6D;3d^44s^1)$ asymptote, where the vanadium atom is in its first excited state only 0.245 eV above its ground state ($M_J$-averaged value).[9] In that case the ground $X^7\Sigma^+$ state is formed mainly through a 2 center-3 electron (2c-3e) interaction leading to a relatively weakly bound system. Of course, the combination $Sc(^4F;3d^24s^1) + V(^6D;3d^44s^1)$, with all electrons uncoupled, should be more favorable for stronger covalent bonding. Unfortunately, the $Sc(^4F)$ state is located 1.427 eV higher than its ground state. Therefore the $Sc(^4F) + V(^6D)$ atomic limit, which lies 1.672 eV above the ground state atoms, cannot form molecular states that are sufficiently bound to become the ground state. Now, returning to the TiV system we find that Ti has its first excited state, $^5F$, significantly lower, at 0.833 eV,[9] which gives an energy gap of 1.051 eV for the $Ti(^5F;3d^34s^1) + V(^6D;3d^44s^1)$ asymptote relative to the ground-state separated atomic limit. It is, therefore, expected to interfere significantly in the formation of low-lying electronic states of TiV. Indeed, as we will see below, many of them, as well as the ground state of TiV, originate from that atomic limit. To make things clearer and also to show the complexity arising from the Ti + V interaction, all Λ–Σ states of TiV resulting from the low-lying atomic asymptotes are given below:

$$Ti(^3F) + V(^4F) \rightarrow {}^{2,4,6}[\Sigma^+(4), \Sigma^-(3), \Pi(6), \Delta(5), \Phi(4), \Gamma(3), H(2), I]$$
(84 states)

$$Ti(^3F) + V(^6D) \rightarrow {}^{4,6,8}[\Sigma^+(2), \Sigma^-(3), \Pi(5), \Delta(4), \Phi(3), \Gamma(2), H]$$
(0.245 eV, 60 states)

$$Ti(^5F) + V(^4F) \rightarrow {}^{2,4,6,8}[\Sigma^+(4), \Sigma^-(3), \Pi(6), \Delta(5), \Phi(4), \Gamma(3), H(2), I]$$
(0.806 eV, 112 states)

$$Ti(^1D) + V(^4F) \rightarrow {}^{4}[\Sigma^+(2), \Sigma^-(3), \Pi(5), \Delta(4), \Phi(3), \Gamma(2), H]$$
(0.871 eV, 20 states)

$$Ti(^3F) + V(^4D) \rightarrow {}^{2,4,6}[\Sigma^+(2), \Sigma^-(3), \Pi(5), \Delta(4), \Phi(3), \Gamma(2), H]$$
(1.026 eV, 60 states)

$$Ti(^5F) + V(^6D) \rightarrow {}^{2,4,6,8,10}[\Sigma^+(2), \Sigma^-(3), \Pi(5), \Delta(4), \Phi(3), \Gamma(2), H]$$
(1.051 eV, 100 states)

*i.e.* a total of 436 $^{2S+1}\Lambda$ electronic states within an asymptotic energy window of ~1 eV. This number increases dramatically if we take into account the spin–orbit coupling (SOC) which, however, is not so important for such light atoms and we believe that considering the Λ–S coupling picture is a very good first-order approach. See also some SOC results discussed at the end of the Results and Discussion section.

From the above it appears that only a robust multireference strategy is appropriate to reliably address this situation. Thus, in what follows, the MRCISD methodology in conjunction with large basis sets was employed in order to calculate potential energy curves (PEC), spectroscopic constants, dipole moments, and binding energies for a total of 45 $^{2S+1}\Lambda$ electronic states of the TiV molecular system. Moreover, a discussion is held with the aim of elucidating the way bonds are formed in the different states of the molecule. Finally, an effort was made to determine the binding energy of the ground and first excited states of TiV as accurately and systematically as possible.

## 2. Computational outline

For all calculated states and corresponding potential energy curves (PEC) the correlation consistent basis sets of quadruple cardinality, cc-pVQZ, were used for both atoms generally contracted to [8s, 7p, 5d, 3f, 2g][10] comprising 186 contracted spherical Gaussians. The choice of the cc-pVQZ basis set for the construction of potential energy curves was made to achieve an acceptable compromise between the quality of results and computational cost (computing time and memory usage).

For the ground and two excited states the triple cc-pVTZ and the quintuple cc-pV5Z basis sets[10] contracted as [7s, 6p, 4d, 2f] and [9s, 8p, 6d, 4f, 3g, 2h], respectively, were also employed at equilibrium geometries. For the scalar relativistic Douglas–Kroll–Hess (DKH)[11,12] calculations we used the same basis sets, cc-pV*n*Z-DK with $n = T, Q, 5$, appropriately contracted.

Our computational approach was based on the internally contracted[13] multireference configuration interaction method, CASSCF + single + double replacements ≡ MRCI. The reference complete active space (CAS) was constructed by distributing the nine valence electrons ($3d^24s^2 + 3d^34s^2$) of TiV to 15 orbitals correlating with the [4s(1) + 3d(5)] × 2 valence space of the Ti and V fragments supplemented with three orbitals of $A_1$, $B_1$, and $B_2$ symmetries (under $C_{2v}$ restrictions) in order to provide greater flexibility to the active space. The size of the resulting CAS spaces under $C_{2v}$ symmetry restrictions were, roughly, $2.3 \times 10^4$ configuration state functions (CSF) for octets, $14.5 \times 10^4$ CSFs (sextets), $4 \times 10^5$ CSFs (quartets), and $4.6 \times 10^5$ CSFs (doublets). During the CASSCF optimization a number of states from all four irreducible representations ($A_1$, $A_2$, $B_1$, $B_2$) were state averaged in order to assure a smooth evolution of the PECs along the internuclear distance and also correct Λ values. More specifically, states from $A_1$ and $A_2$ irreps were averaged for the description of Σ, Δ, Γ molecular $C_{\infty v}$ symmetries whilst $B_1$ and $B_2$ were used for the Π, Φ, and H states.

In the present calculations we did not consider the known double d-shell effect, (see for instance ref. 14) because it doesn't seem important for the Ti and V atoms. For example the $[V(^4F) \leftarrow V(^6D)]$ energy gap is very accurately predicted with the present computational scheme (*vide infra*).

The subsequent MRCI expansions contain $0.24–2.54 \times 10^9$ uncontracted CSFs internally contracted[13] to $9–55 \times 10^6$ CSFs.

At all stages of our calculations, MCSCF and MRCI, the convergence thresholds were $10^{-7}$ for energies and $10^{-6}$ for the coefficients gradient or the density.

Size non-extensivity was taken into account by applying the multireference Davidson correction[15] for unlinked quadruples, MRCI + Q.

Spectroscopic constants were extracted by numerically solving the nuclear Schrödinger equation using a Numerov procedure with a code developed in our laboratory and employing the masses of the $^{48}Ti$ and $^{51}V$ isotopes.

Table 1 Energy $E$ ($E_h$), bond length $r_e$ (Å), binding energies $D_e$, $D_0$ (kcal mol$^{-1}$), Harmonic frequency $\omega_e$ (cm$^{-1}$), anharmonicity constant $\omega_e x_e$ (cm$^{-1}$), centrifugal distortion constant $\bar{D}e$ (cm$^{-1}$), rotation-vibration coupling constant $a_e$ (cm$^{-1}$), net Mulliken charge $q_{Ti}$ (e) on Ti, dipole moment $\mu$ (Debye) and energy separation $T_e$ (cm$^{-1}$) for 45 low-lying electronic states of TiV at the MRCI(+Q)/cc-pVQZ level of theory

| Method | $-E$ | $r_e$ | $D_e$[a] | $D_0$[a] | $\omega_e$ | $\omega_e x_e$ | $\bar{D}_e$ ($\times 10^{-7}$) | $a_e$ ($\times 10^{-3}$) | $q_{Ti}$ | $\mu$ | $T_e$ |
|---|---|---|---|---|---|---|---|---|---|---|---|
| **Xs $^4\Sigma^-$** | | | | | | | | | | | |
| MRCI | 1791.46830 | 1.897 | 29.3 | 28.8 | 391 | 1.576 | 1.78 | 1.37 | −0.08 | 0.37 | 0 |
| MRCI + Q (secondary minimum) | 1791.4796 | 1.900 | 31.0 | 30.5 | 377 | 0.846 | 1.80 | 1.38 | | | 0 |
| MRCI | 1791.43625 | 2.729 | 9.2 | 9.0 | 173 | 3.620 | 1.10 | 0.29 | +0.04 | 0.13 | 7034 |
| MRCI + Q | 1791.4483 | 2.708 | 11.4 | 11.2 | 178 | 3.300 | 1.20 | 0.61 | | | 6869 |
| **1 $^2\Delta$** | | | | | | | | | | | |
| MRCI | 1791.46407 | 1.920 | 27.4 | 26.8 | 476 | 8.887 | 1.12 | 1.52 | −0.12 | 0.23 | 928 |
| MRCI + Q | 1791.4739 | 1.936 | 28.3 | 27.7 | 496 | 7.269 | 1.03 | 2.21 | | | 1251 |
| **2 $^2\Gamma$** | | | | | | | | | | | |
| MRCI | 1791.45268 | 1.903 | 20.2 | 19.8 | 271 | 1.721 | 3.19 | 3.15 | −0.09 | 0.69 | 3428 |
| MRCI + Q | 1791.4642 | 1.903 | 22.2 | 21.8 | 307 | 0.832 | 2.73 | 1.95 | | | 2941 |
| **3 $^2\Sigma^+$** | | | | | | | | | | | |
| MRCI | 1791.45207 | 1.903 | 19.6 | 19.2 | 239 | 2.654 | 4.70 | 9.61 | −0.13 | 0.73 | 3562 |
| MRCI + Q | 1791.4636 | 1.903 | 21.5 | 21.0 | 288 | 7.102 | 3.05 | −1.08 | | | 3512 |
| **4 $^4\Pi$** | | | | | | | | | | | |
| MRCI | 1791.44998 | 1.993 | 17.9 | 17.3 | 360 | 11.990 | 1.56 | 2.44 | −0.08 | 0.21 | 4021 |
| MRCI + Q (secondary minimum) | 1791.4641 | 2.028 | 21.4 | 20.1 | 337 | 8.860 | 1.61 | 1.57 | | | 3402 |
| MRCI | 1791.43776 | 2.686 | 10.2 | 10.0 | 164 | 3.630 | 1.35 | 0.61 | 0.02 | 0.03 | 6703 |
| MRCI + Q | 1791.4491 | 2.695 | 12.0 | 11.7 | 163 | 8.010 | 0.43 | −1.27 | | | 6694 |
| **5 $^2\Sigma^-$** | | | | | | | | | | | |
| MRCI | 1791.44691 | 1.827 | 16.4 | 15.8 | 429 | 9.781 | 2.32 | −0.82 | −0.05 | 0.24 | 4695 |
| MRCI + Q | 1791.4580 | 1.827 | 17.9 | 17.4 | 387 | 2.425 | 2.69 | −0.33 | | | 4741 |
| **6 $^8\Delta$** | | | | | | | | | | | |
| MRCI | 1791.44595 | 2.644 | 20.9 | 20.6 | 219 | 8.992 | 0.50 | 0.13 | −0.05 | 0.34 | 4905 |
| MRCI + Q | 1791.4583 | 2.630 | 25.6 | 25.3 | 231 | 7.309 | 0.37 | −0.14 | | | 4675 |
| **7 $^4\Delta$** | | | | | | | | | | | |
| MRCI | 1791.44440 | 2.163 | 14.5 | 14.2 | 185 | 1.312 | 3.48 | −2.55 | −0.07 | 0.23 | 5245 |
| MRCI + Q | 1791.4545 | 2.171 | 15.4 | 15.1 | 180 | 1.189 | 3.85 | −0.03 | | | 5509 |
| **8 $^8$H** | | | | | | | | | | | |
| MRCI | 1791.44124 | 2.801 | 17.9 | 17.6 | 197 | 0.798 | 0.63 | 0.37 | −0.01 | 0.34 | 5939 |
| MRCI + Q | 1791.4526 | 2.788 | 22.0 | 21.7 | 203 | 0.346 | 0.69 | 0.47 | | | 5926 |
| **9 $^6\Pi$** | | | | | | | | | | | |
| MRCI | 1791.44082 | 2.641 | 12.3 | 12.1 | 126 | 4.884 | 1.48 | −2.92 | −0.01 | 0.08 | 6031 |
| MRCI + Q | 1791.4519 | 2.641 | 14.0 | 13.8 | 116 | 3.953 | 1.95 | −5.05 | | | 6079 |
| **10 $^6$H** | | | | | | | | | | | |
| MRCI | 1791.44080 | 2.707 | 12.3 | 12.0 | 171 | 0.483 | 1.26 | 0.23 | 0.00 | 0.14 | 6036 |
| MRCI + Q | 1791.4518 | 2.715 | 13.9 | 13.7 | 176 | 1.925 | 0.63 | 0.03 | | | 6101 |
| **11 $^8\Pi$** | | | | | | | | | | | |
| MRCI | 1791.43999 | 2.812 | 17.1 | 16.8 | 186 | 0.951 | 0.53 | 0.28 | 0.00 | 0.36 | 6213 |
| MRCI + Q | 1791.4515 | 2.791 | 21.3 | 21.0 | 191 | 0.711 | 1.22 | 32.5 | | | 6167 |
| **12 $^2\Pi$** | | | | | | | | | | | |
| MRCI | 1791.43942 | 2.049 | 11.2 | 10.8 | 327 | 0.926 | 1.59 | 0.36 | −0.14 | 0.83 | 6338 |
| MRCI + Q | 1791.4500 | 2.069 | 12.5 | 12.1 | 275 | 5.973 | 2.10 | 2.20 | | | 6496 |
| **13 $^2$H** | | | | | | | | | | | |
| MRCI | 1791.43894 | 2.066 | 10.9 | 10.5 | 288 | 10.977 | 1.76 | 3.67 | −0.15 | 0.83 | 6444 |
| MRCI + Q | 1791.4494 | 2.089 | 12.1 | 11.7 | 269 | 4.729 | 2.29 | 1.13 | | | 6628 |
| **14 $^6\Pi$** | | | | | | | | | | | |
| MRCI | 1791.43835 | 2.666 | 10.8 | 10.6 | 160 | −0.304 | 1.60 | 0.23 | −0.02 | 0.01 | 6573 |
| MRCI + Q | 1791.4497 | 2.682 | 12.5 | 12.3 | 163 | −0.496 | 1.31 | 0.22 | | | 6562 |
| **15 $^6\Sigma^+$** | | | | | | | | | | | |
| MRCI | 1791.43828 | 2.677 | 10.5 | 10.3 | 127 | 1.058 | 2.36 | −0.20 | 0.01 | 0.11 | 6589 |
| MRCI + Q | 1791.4505 | 2.654 | 12.8 | 12.6 | 124 | 2.445 | 2.38 | −0.07 | | | 6387 |
| **16 $^8\Sigma^+$** | | | | | | | | | | | |
| MRCI | 1791.43775 | 2.800 | 15.7 | 15.5 | 189 | 7.059 | 0.01 | −0.28 | 0.00 | 0.60 | 6705 |
| MRCI + Q | 1791.4490 | 2.750 | 19.8 | 19.5 | 189 | 3.019 | 0.85 | −0.76 | | | 6716 |
| **17 $^6\Phi$** | | | | | | | | | | | |
| MRCI | 1791.43771 | 2.690 | 10.4 | 10.2 | 163 | 0.921 | 1.26 | 0.16 | 0.00 | 0.15 | 6714 |
| MRCI + Q | 1791.4491 | 2.682 | 12.2 | 11.9 | 165 | 0.769 | 1.24 | 0.12 | | | 6694 |
| **18 $^4$H** | | | | | | | | | | | |
| MRCI | 1791.43757 | 2.692 | 10.2 | 9.9 | 163 | 0.119 | 1.14 | 0.38 | 0.02 | 0.03 | 6744 |
| MRCI + Q | 1791.4489 | 2.703 | 11.9 | 11.6 | 164 | 0.649 | 1.20 | 0.09 | | | 6738 |
| **19 $^6\Sigma^-$** | | | | | | | | | | | |
| MRCI | 1791.43751 | 2.717 | 10.0 | 9.8 | 154 | 7.066 | 1.32 | 1.94 | 0.01 | 0.17 | 6758 |
| MRCI + Q | 1791.4495 | 2.709 | 12.2 | 11.9 | 171 | 1.437 | 1.09 | 0.36 | | | 6606 |
| **20 $^2\Delta$** | | | | | | | | | | | |
| MRCI | 1791.43736 | 2.205 | 10.7 | 10.4 | 237 | 4.180 | 1.80 | 0.92 | −0.08 | 0.18 | 6791 |
| MRCI + Q | 1791.4496 | 2.226 | 12.6 | 12.3 | 202 | 8.050 | 2.38 | 2.92 | | | 6584 |
| **21 $^6\Gamma$** | | | | | | | | | | | |
| MRCI | 1791.43704 | 2.717 | 9.7 | 9.5 | 177 | 6.741 | 0.84 | 0.32 | 0.02 | 0.16 | 6861 |
| MRCI + Q | 1791.4489 | 2.709 | 11.8 | 11.5 | 180 | 6.913 | 0.98 | 0.84 | | | 6738 |

Table 1 (*continued*)

| Method | $-E$ | $r_e$ | $D_e$[a] | $D_0$[a] | $\omega_e$ | $\omega_e x_e$ | $\bar{D}_e$ ($\times 10^{-7}$) | $a_e$ ($\times 10^{-3}$) | $q_{Ti}$ | $\mu$ | $T_e$ |
|---|---|---|---|---|---|---|---|---|---|---|---|
| **22 $^8\Pi$** | | | | | | | | | | | |
| MRCI | 1791.43698 | 2.820 | 15.2 | 15.0 | 184 | 0.984 | 0.41 | 0.70 | 0.00 | 0.40 | 6874 |
| MRCI + Q | 1791.4485 | 2.800 | 19.4 | 19.1 | 197 | 2.750 | 0.57 | 0.73 | | | 6826 |
| **23 $^8\Gamma$** | | | | | | | | | | | |
| MRCI | 1791.43690 | 2.822 | 15.2 | 15.0 | 195 | 2.249 | 0.61 | 1.06 | 0.00 | 0.58 | 6892 |
| MRCI + Q | 1791.4480 | 2.800 | 19.2 | 18.9 | 202 | 2.496 | 0.57 | 0.84 | | | 6935 |
| **24 $^4\Phi$** | | | | | | | | | | | |
| MRCI | 1791.43677 | 2.628 | 9.9 | 9.7 | 139 | 0.748 | 2.01 | −0.96 | 0.00 | 0.04 | 6920 |
| MRCI + Q | 1791.4487 | 2.620 | 11.8 | 11.6 | 155 | 8.126 | 1.07 | −1.01 | | | 6782 |
| **25 $^8\Sigma^-$** | | | | | | | | | | | |
| MRCI | 1791.43676 | 2.761 | 15.1 | 14.8 | 196 | 0.756 | 0.66 | 0.26 | 0.00 | 0.52 | 6922 |
| MRCI + Q | 1791.4480 | 2.753 | 19.1 | 18.7 | 203 | 0.471 | 0.63 | 0.11 | | | 6935 |
| **26 $^4\Pi$** | | | | | | | | | | | |
| MRCI | 1791.43658 | 2.653 | 9.8 | 9.6 | 224 | 8.991 | 0.61 | −1.03 | 0.02 | 0.03 | 6962 |
| MRCI + Q | 1791.4485 | 2.645 | 11.7 | 11.5 | 220 | 8.548 | 0.73 | −0.67 | | | 6826 |
| **27 $^4\Gamma$** | | | | | | | | | | | |
| MRCI | 1791.43615 | 2.748 | 9.2 | 9.0 | 164 | −0.127 | 1.08 | 1.50 | −0.14 | 0.87 | 7056 |
| MRCI + Q | 1791.4483 | 2.726 | 11.4 | 11.2 | 188 | 5.774 | 0.78 | −1.10 | | | 6870 |
| **28 $^8\Phi$** | | | | | | | | | | | |
| MRCI | 1791.43606 | 2.851 | 14.7 | 14.4 | 174 | 0.314 | 0.76 | 0.44 | 0.00 | 0.44 | 7076 |
| MRCI + Q | 1791.4474 | 2.835 | 18.7 | 18.4 | 182 | 0.821 | 0.74 | 0.75 | | | 7067 |
| **29 $^4\Sigma^+$** | | | | | | | | | | | |
| MRCI | 1791.43603 | 2.734 | 9.1 | 8.8 | 170 | 2.713 | 0.93 | 0.88 | −0.16 | 0.87 | 7082 |
| MRCI + Q | 1791.4481 | 2.717 | 11.2 | 11.0 | 174 | 3.647 | 0.75 | 1.69 | | | 6913 |
| **30 $^2\Phi$** | | | | | | | | | | | |
| MRCI | 1791.43590 | 2.057 | 9.0 | 8.6 | 293 | 7.000 | 1.92 | 1.89 | −0.11 | 0.83 | 7111 |
| MRCI + Q | 1791.4467 | 2.092 | 10.4 | 10.0 | 283 | 8.049 | 1.93 | 1.00 | | | 7221 |
| **31 $^8\Delta$** | | | | | | | | | | | |
| MRCI | 1791.43452 | 2.881 | 13.7 | 13.5 | 181 | 0.602 | 0.60 | 0.24 | 0.00 | 0.66 | 7414 |
| MRCI + Q | 1791.4460 | 2.857 | 17.9 | 17.6 | 186 | 0.614 | 0.68 | 0.74 | | | 7374 |
| **32 $^6\Delta$** | | | | | | | | | | | |
| MRCI | 1791.43433 | 2.748 | 8.0 | 7.8 | 171 | 4.329 | 0.91 | 0.80 | 0.02 | 0.16 | 7456 |
| MRCI + Q | 1791.4466 | 2.741 | 10.4 | 10.1 | 177 | 3.338 | 0.96 | 0.06 | | | 7243 |
| **33 $^2\Pi$** | | | | | | | | | | | |
| MRCI | 1791.43419 | 2.631 | 8.0 | 7.6 | 226 | 7.594 | 0.75 | 2.16 | 0.03 | 0.04 | 7486 |
| MRCI + Q | 1791.4455 | 2.632 | 9.6 | 9.3 | 216 | 5.825 | 0.82 | 0.79 | | | 7484 |
| **34 $^4\Pi$** | | | | | | | | | | | |
| MRCI | 1791.43257 | 2.419 | 7.0 | 6.8 | 141 | 1.420 | 2.06 | −0.68 | −0.10 | 0.07 | 7842 |
| MRCI + Q | 1791.4433 | 2.419 | 8.6 | 8.3 | 83 | −9.138 | 4.48 | −2.34 | | | 7967 |
| **35 $^4\Sigma^-$** | | | | | | | | | | | |
| MRCI | 1791.43214 | 2.699 | 6.7 | 6.4 | 179 | — | — | — | 0.03 | 0.07 | 7936 |
| MRCI + Q | 1791.4444 | 2.725 | 9.0 | 8.8 | 125 | — | — | — | | | 7726 |
| **36 $^4$H** | | | | | | | | | | | |
| MRCI | 1791.43187 | 2.655 | 4.6 | 4.3 | 178 | 0.767 | 1.15 | 0.51 | 0.01 | 0.11 | 7995 |
| MRCI + Q | 1791.4430 | 2.652 | 4.5 | 4.2 | 160 | −1.105 | 1.08 | 0.93 | | | 8033 |
| **37 $^4\Gamma$** | | | | | | | | | | | |
| MRCI | 1791.43183 | 2.702 | 6.5 | 6.2 | 180 | 2.084 | 0.53 | 0.29 | 0.03 | 0.05 | 8004 |
| MRCI + Q | 1791.4457 | 2.705 | 9.8 | 9.6 | 186 | 2.741 | 1.02 | 0.17 | | | 7440 |
| **38 $^6\Delta$** | | | | | | | | | | | |
| MRCI | 1791.43176 | 2.733 | 6.4 | 6.2 | 130 | 1.224 | 1.90 | 0.92 | −0.03 | 0.17 | 8020 |
| MRCI + Q | 1791.4443 | 2.725 | 8.9 | 8.7 | 157 | 7.379 | 1.34 | 0.72 | | | 7747 |
| **39 $^2\Sigma^-$** | | | | | | | | | | | |
| MRCI | 1791.43001 | 2.063 | 8.3 | 7.7 | 422 | 9.835 | 0.89 | 0.44 | −0.10 | 0.73 | 8404 |
| MRCI + Q | 1791.4428 | 2.053 | 9.6 | 9.1 | 411 | 4.829 | 1.21 | 1.41 | | | 8077 |
| **40 $^4\Pi$** | | | | | | | | | | | |
| MRCI | 1791.43001 | 2.633 | 4.5 | 4.2 | 164 | 0.714 | 1.43 | 0.91 | −0.01 | 0.10 | 8404 |
| MRCI + Q | 1791.4418 | 2.654 | 4.0 | 3.8 | 164 | 0.426 | 1.28 | 0.26 | | | 8296 |
| **41 $^8\Pi$** | | | | | | | | | | | |
| MRCI | 1791.42962 | 2.938 | 10.7 | 10.4 | 160 | 3.980 | 0.80 | 0.41 | −0.01 | 0.48 | 8489 |
| MRCI + Q | 1791.4420 | 2.875 | 15.4 | 15.1 | 193 | 3.264 | 0.59 | 0.40 | | | 8252 |
| **42 $^8\Sigma^+$** | | | | | | | | | | | |
| MRCI | 1791.42754 | 2.985 | 9.4 | 9.2 | 152 | 7.556 | 0.63 | 2.15 | −0.01 | 0.71 | 8946 |
| MRCI + Q | 1791.4389 | 2.929 | 13.4 | 13.2 | 184 | 7.119 | 0.38 | −1.62 | | | 8933 |
| **43 $^8\Gamma$** | | | | | | | | | | | |
| MRCI | 1791.42732 | 3.081 | 9.3 | 9.0 | 149 | −1.920 | 1.04 | −0.53 | −0.02 | 0.67 | 8994 |
| MRCI + Q | 1791.4382 | 2.993 | 13.0 | 12.8 | 159 | −0.881 | 0.65 | 0.36 | | | 9086 |
| **44 $^8\Delta$** | | | | | | | | | | | |
| MRCI | 1791.42650 | 2.993 | 8.7 | 8.5 | 149 | 3.433 | 0.78 | 0.82 | 0.00 | 0.41 | 9174 |
| MRCI + Q | 1791.4378 | 2.937 | 12.8 | 12.5 | 182 | 1.843 | 0.59 | 0.31 | | | 9174 |

[a] Binding energies with respect to Ti($^3$F) + V($^6$D) for all octet states and with respect to Ti($^3$F) + V($^4$F) for all other states.

All calculations were carried out with the MOLPRO2025.1-4 program.[16,17]

## 3. Results and discussion

Table 1 collects the numerical data obtained for 45 electronic states of TiV while Fig. 1, 3, 4 and 5 display the corresponding PECs for spin multiplicities 4, 2, 6, and 8, respectively. The different states are numbered in ascending order of their absolute electronic energies as obtained at the MRCI level. In some cases of near-degeneracy the ordering based on the MRCI energies is reversed at the MRCI + Q level.

From Table 1, it is clear that the ground state of TiV is of $X^4\Sigma^-$ symmetry with a $^2\Delta$ state lying slightly higher. Thus, we discuss first quartet states, then doublets, and finally sextets and octets. We conclude this section with a discussion on the binding energies of the $X^4\Sigma^-$, $1^2\Delta$, and $4^4\Pi$ electronic states.

### 3.1 Quartets

We first present all quartet states studied in this work, as the TiV ground state was found to be a $^4\Sigma^-$, in complete agreement with the observation of Van Zee and Weltner Jr.[1]

In Fig. 1a, we can see its PEC, which adiabatically correlates with the ground atomic states Ti($^3$F) + V($^4$F). This curve has a rather unusual shape, indicative of successive avoided crossings. Therefore, it will be enlightening to explore the nature of its morphology as a function of the interatomic Ti–V separation. As stated in the Introduction section, the ground atomic states Ti($^3$F;3d$^2$4s$^2$) + V($^4$F;3d$^3$4s$^2$) can only lead to weak vdW interactions. Indeed, at $r$(Ti–V) = ~3.40 Å, we observe a very shallow minimum of ~3 kcal mol$^{-1}$. Then, at this point, an abrupt change occurs, resulting in the formation of a relatively shallow potential well with a local minimum at $r$(Ti–V) = 2.729 (2.708) Å and a binding energy $D_0^0$ = 9.0 (11.2) kcal mol$^{-1}$ at the MRCI(+Q)/cc-pVQZ level, Table 1. This is apparently the result of an avoided crossing with an incoming curve of same symmetry that stems from a higher atomic asymptote. This is clearly illustrated in Fig. 1a, where it is shown that this local minimum non-adiabatically traces its origin to the first atomic asymptote Ti($^3$F) + V($^6$D), lying 0.245 eV above the ground-state atomic limit. This quasi-diabatic curve (grey line) was produced by a CASSCF reference accidentally locked into this minimum's electronic configuration. This means that, at the crossing point, the MCSCF reference, instead of following the lowest adiabatic path, continues onto the higher asymptotic limit, which corresponds to the equilibrium electronic configuration. Furthermore, inspection of the electronic wavefunction shows an *in situ* electronic distribution corresponding to Ti(3d$^2$4s$^2$)-V(3d$^4$4s$^1$). The bonding occurs, mainly, through a 2 center-3 electron (2c-3e) interaction of the Ti(4s$^2$)–(4s$^1$)V electrons, with minor contributions from the 3d electrons, resulting in a weak bond. We will discuss this binding mode further in the discussion of sextet and octet states.

Now, moving further left on the same adiabatic curve, we come across a second sharp change at $r$(Ti–V) = 2.40 Å, obviously a second avoided crossing, leading to a much deeper potential energy well. It forms the global minimum, hence the

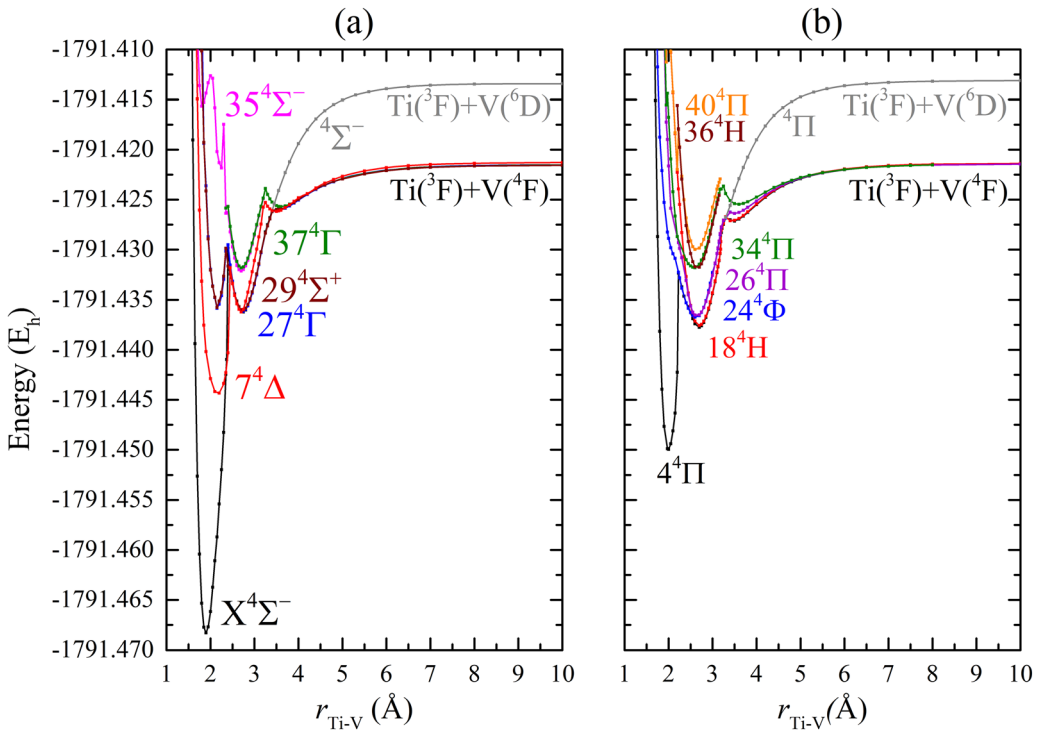


Fig. 1 Potential energy curves of the thirteen lowest quartet states of TiV at the MRCI/cc-pVQZ level of theory: (a) $X^4\Sigma^-$, $7^4\Delta$, $27^4\Gamma$, $29^4\Sigma^+$, $35^4\Sigma^-$, $37^4\Gamma$ and (b) $4^4\Pi$, $18^4$H, $24^4\Phi$, $26^4\Pi$, $34^4\Pi$, $36^4$H, $40^4\Pi$.

ground $X^4\Sigma^-$ state of TiV. Thus, we are going to investigate it in detail.

The equilibrium TiV($X^4\Sigma^-$) MRCI wavefunction is dominated by the configuration

$$|(\text{core})1\sigma^2 2\sigma^1 1\pi^4 1\delta_+^1 1\delta_-^1\rangle$$

(where only valence orbitals are counted) with a coefficient of 0.83. This electronic configuration is identical with the one proposed in ref. 1 on the basis of ESR observations, see Inroduction. The corresponding atomic Mulliken electronic distributions at equilibrium are:

$$4s^{1.14}4p_z^{0.00}4p_x^{0.06}4p_y^{0.06}3d_{z^2}^{0.38}3d_{xz}^{0.93}3d_{yz}^{0.93}3d_{x^2-y^2}^{0.29}3d_{xy}^{0.29}\Big/\text{Ti}(-0.08)$$

$$4s^{0.86}4p_z^{0.00}4p_x^{0.05}4p_y^{0.05}3d_{z^2}^{0.62}3d_{xz}^{0.96}3d_{yz}^{0.96}3d_{x^2-y^2}^{0.71}3d_{xy}^{0.71}\Big/\text{V}(+0.08)$$

These populations coupled to the active orbitals participating in the leading configuration (Fig. 2) suggest a bonding situation which can be depicted by Scheme 1.

In this Scheme, the 3d orbitals are represented by over-extended sticks in order to clearly show the formal interactions between them. It becomes apparent from the overall electronic arrangement that the *in situ* atomic states correspond to the Ti($^5$F) + V($^6$D) excited asymptote located 1.051 eV (see Inroduction) above the ground separated atomic limit. A significant stabilization takes place through a formally 3-bond + 3-half-bond, formation, making this configuration the ground state of

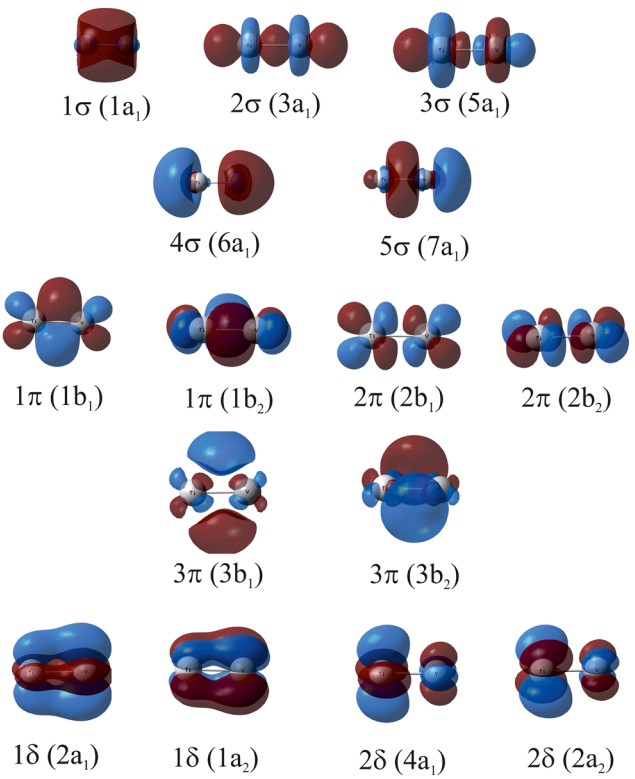


Fig. 2 Illustration of the 15 natural orbitals participating in the CASSCF and MRCI active space for the TiV($X^4\Sigma^-$) state at equilibrium. Their shapes are practically the same for all other states studied.

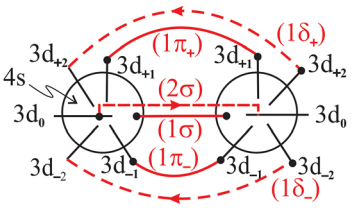


$\equiv$ TiV($X^4\Sigma^-$)

Ti($^5$F;$M_L$= 0) V($^6$D;$M_L$= 0)

Scheme 1

TiV after crossing all states of the same symmetry that arise from intermediate atomic channels shown in the Introduction section.

The equilibrium bond length was found $r_e$ = 1.900 Å. This is close to the MCSCF result, $r_e$ = 1.86 Å, of ref. 8 but larger by ~0.1 Å than the DFT findings of ref. 5 and 6. The binding energy with respect to the ground state adiabatic limit was computed $D_0^0$ = 30.5 kcal mol$^{-1}$ = 1.323 eV at the MRCI + Q/cc-pVQZ level of theory, Table 1. This is much lower than the most recent experimental value, $D_0^0$ = 2.068 eV, of Spain and Morse.[4] As of the DFT values of 5.88 eV[5] and 2.78 eV,[6] they are deemed rather excessive. We will return to this binding energy problem with a dedicated section at the end of this discussion.

On Table 1, are also reported spectroscopic constants and the dipole moment of TiV($X^4\Sigma^-$), as they were computed at the MRCI(+Q)/cc-pVQZ level. We note that our harmonic frequency, $\omega_e$ = 377 cm$^{-1}$, is much lower than the DFT value, $\omega_e$ = 562 cm$^{-1}$, of Gutzev *et al.*[6] The very low value of the dipole moment, $\mu$ = 0.37 D, reflects a very small overall charge transfer, in agreement with Scheme 1 and the corresponding Mulliken populations.

We can see from Fig. 1 that the states $4^4\Pi$, $7^4\Delta$, $27^4\Gamma$, and $29^4\Sigma^+$, also have PECs exhibiting the same double-well aspect as the ground state, with a first minimum at ~2.7–2.8 Å and a second one at around 1.9–2.0 Å. Just like for the ground state, we find out that the first minima originate from the first excited atomic channel Ti($^3$F) + V($^6$D), while the second ones come from the Ti($^5$F) + V($^6$D) asymptote. All states with a single minimum at ~2.70 Å correspond to Ti($^3$F) + V($^6$D).

We are going, now, to deal with the $4^4\Pi$ state, Fig. 1b, which is suitable (dipole allowed) for a spectroscopic study of TiV. Its PEC has same shape as the one of the ground state. The global minimum is at $r_e$ = 1.993 (2.028) Å with binding energy $D_0^0$ = 17.3 (20.1) kcal mol$^{-1}$ at the MRCI(+Q)/cc-pVQZ level. Its equilibrium wavefunction, although of a somewhat multireference nature, is mainly characterized by the configuration

$$|(\text{core})1\sigma^2 2\sigma^1 1\pi^3 1\delta_+^1 1\delta_-^1\rangle$$

with a coefficient of 0.75. Taking into account and the atomic Mulliken populations ($B_1$ component):

$$4s^{1.12}4p_z^{0.04}4p_x^{0.08}4p_y^{0.06}3d_{z^2}^{0.86}3d_{xz}^{0.89}3d_{yz}^{0.41}3d_{x^2-y^2}^{0.31}3d_{xy}^{0.31}\Big/\text{Ti}(-0.08)$$

$$4s^{0.80}4p_z^{0.02}4p_x^{0.07}4p_y^{0.06}3d_{z^2}^{0.96}3d_{xz}^{0.92}3d_{yz}^{0.55}3d_{x^2-y^2}^{0.72}3d_{xy}^{0.72}\Big/\text{V}(+0.08)$$

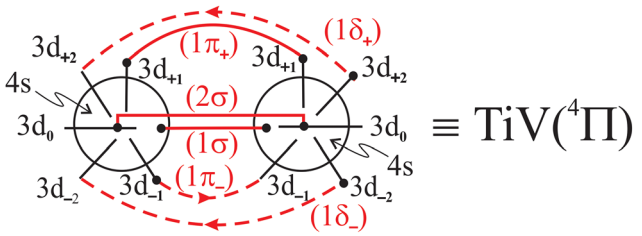


Scheme 2

the binding can be described by Scheme 2, from which it is clear again, that the two atoms are in their excited Ti($^5$F) + V($^6$D) states.

We have calculated for this state an excitation energy $T_e$ = 4021 (3402) cm$^{-1}$ at the MRCI(+Q)/cc-pVQZ level (Table 1); thus it could be accessed spectroscopically in the infrared.

### 3.2 Doublets

Fig. 3 shows potential energy curves for 10 doublet states. We can see from this figure and also from Table 1 that the first three excited states of TiV are the $1^2\Delta$, $2^2\Gamma$, and $3^2\Sigma^+$ doublets, with the $1^2\Delta$ state being located energetically very close to the ground state $X^4\Sigma^-$. We have computed for this state $T_e$ = 928 (1251) cm$^{-1}$ at the MRCI(+Q)/cc-pVQZ level and a bondlength $r_e$ = 1.920 (1.936) Å (Table 1). The proximity of this state to the ground state raises some doubt as to what the true ground state of the molecule is and whether it might change at a higher computational level. However, as we will see below, this energy difference persists at higher levels of theory. Its equilibrium MRCI wavefunction has one leading configuration, *i.e.*

$$|(^2\Delta\rangle \sim 0.80|(\text{core})1\sigma^2 2\sigma^1 1\pi^4 1\delta^1\rangle$$

which combined with the following Mulliken atomic populations ($A_1$ component):

$$4s^{1.14}4p_z^{0.08}4p_x^{0.08}4p_y^{0.08}3d_{z^2}^{0.83}3d_{xz}^{0.89}3d_{yz}^{0.89}3d_{x^2-y^2}^{0.10}3d_{xy}^{0.03}\Big/\text{Ti}(-0.12)$$

$$4s^{0.80}4p_z^{0.04}4p_x^{0.07}4p_y^{0.07}3d_{z^2}^{1.05}3d_{xz}^{0.96}3d_{yz}^{0.96}3d_{x^2-y^2}^{0.90}3d_{xy}^{0.03}\Big/\text{V}(+0.12)$$

lead to a binding mode illustrated in Scheme 3. From this scheme it is clear that the *in situ* atomic states are Ti($^5$F; $M_L$ = 0) + V($^6$D; $M_L$ = ±2). The $1^2\Delta$ state resembles the ground state (Scheme 1) with the only difference being that one δ electron has moved to the σ frame to form a 2-electron bond. Its potential energy curve suffers an avoided crossing with the $20^2\Delta$ state (Fig. 3a) at $r$(Ti–V) = ~2.40 Å, so it forms a shelf in the region 2.40–3.00 Å before crossing the curve coming from the ground state asymptote.

Other doublet curves have the same double-well profile as described for the quartets (*vide supra*). The rationalization of this feature is the same as for the latter, and is omitted.

In concluding this section, we wish to remark that the first excited state of TiV is $1^2\Delta$, in contrast to ref. 6, which claims that it is a $^2\Gamma$. The latter lies higher in energy and is nearly degenerate with a $^2\Sigma^+$ state (Table 1).

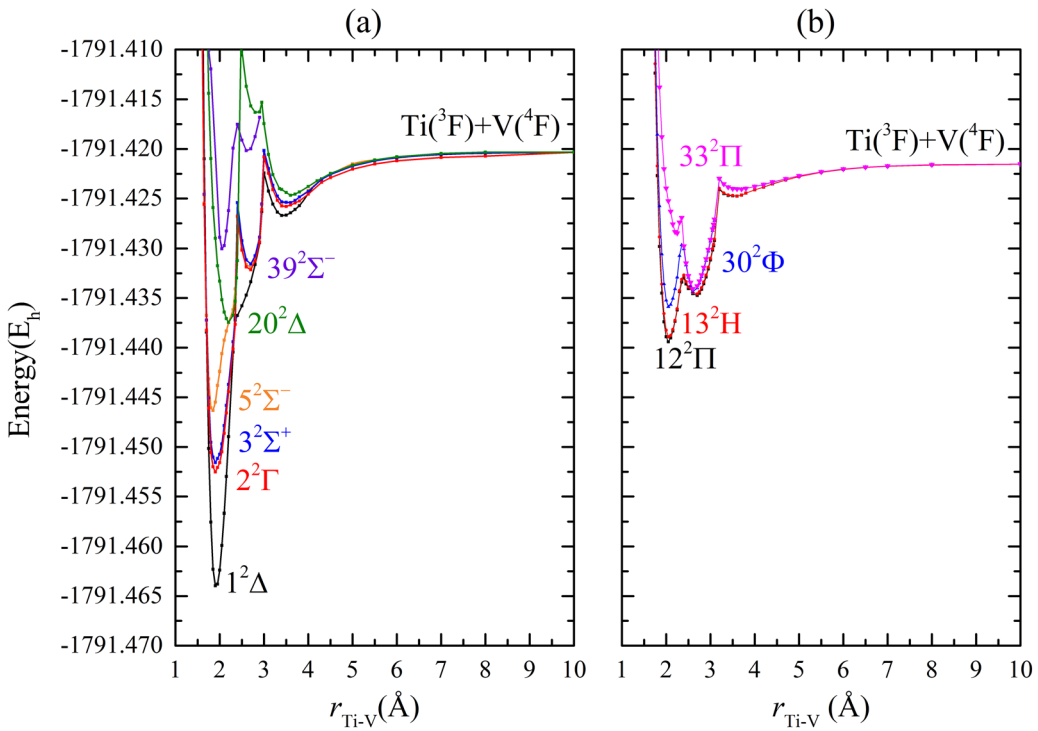


Fig. 3 Potential energy curves of the ten lowest doublet states of TiV at the MRCI/cc-pVQZ level of theory: (a) $1^2\Delta$, $2^2\Gamma$, $3^2\Sigma^+$, $5^2\Sigma^-$, $20^2\Delta$, $39^2\Sigma^-$ and (b) $12^2\Pi$, $13^2$H, $30^2\Phi$, $33^2\Pi$.

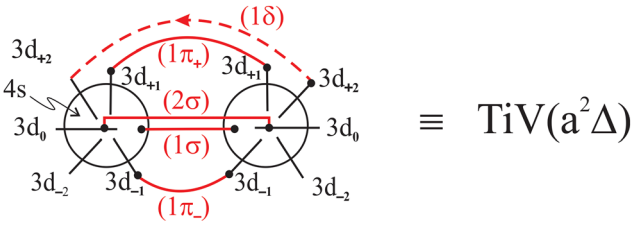


Scheme 3

### 3.3 Sextets and octets

We discuss sextet and octet states together in this section because, as we will see, they all originate from the same asymptote, namely Ti($^3$F) + V($^6$D). The corresponding potential energy curves are shown in Fig. 4 and 5 for sextets and octets, respectively. We observe that, unlike the quartets and doublets, they all exhibit single minima in the vicinity of 2.70–2.80 Å. All octet PECs adiabatically correlate with the Ti($^3$F) + V($^6$D) asymptotic channel since the ground atomic states cannot yield such a spin multiplicity. However, the sextet states adiabatically go to the ground-state atomic limit after suffering avoided crossings at about $r$(Ti–V) = 3.50 Å (Fig. 4). All states have relatively weak binding energies ranging from ~15–25 kcal mol$^{-1}$ (Table 1). As mentioned before, this happens because bonding occurs primarily through a 2c-3e interaction between the more spatially extended 4s orbitals, namely Ti(4s$^2$)–(4s$^1$)V, supplemented by additional weak 3d–3d interactions. As an illustrative example, we will consider the 6$^8$Δ state. At equilibrium, its MRCI wavefunction, although multireference in character, is dominated by the following configuration

$$|(\text{core})1\sigma^2 2\sigma^1 3\sigma^1 1\pi_+^1 1\pi_-^1 1\delta_+^1 1\delta_-^1 2\delta^1\rangle$$

with a coefficient 0.65. The corresponding atomic Mulliken populations ($A_1$ component) are:

$$4s^{1.33}4p_z^{0.27}4p_x^{0.06}4p_y^{0.06}3d_{z^2}^{0.45}3d_{xz}^{0.43}3d_{yz}^{0.43}3d_{x^2-y^2}^{0.97}3d_{xy}^{0.05}\Big/\text{Ti}(-0.05)$$

$$4s^{1.06}4p_z^{0.16}4p_x^{0.05}4p_y^{0.05}3d_{z^2}^{0.68}3d_{xz}^{0.51}3d_{yz}^{0.51}3d_{x^2-y^2}^{0.95}3d_{xy}^{0.98}\Big/\text{V}(+0.05)$$

From these findings we infer the binding mode of Scheme 4. In this scheme the 2c–3e interaction is represented as a two-electron σ-bond with the third electron promoted to a non-bonding orbital (3σ$^1$) (symbolized by an up arrow). This type of bonding is supplemented by additional 3d-3d half-bond interactions (dashed lines) finally yielding a binding energy $D_e$ = 25.6 kcal mol$^{-1}$ relative to the Ti($^3$F) + V($^6$D) asymptote (Table 1). All other octet states depicted in Fig. 5, arise from different arrangements of the 3d electrons while the overall bonding motif remains unchanged. It is interesting to note here that the ground X$^7\Sigma^+$ state of ScV is formed through a similar mechanism and has a comparable binding energy $D_e$ = 28 kcal mol$^{-1}$.[8]

Now, turning to the sextet states, we see from Fig. 4 that they all present minima at about $r$(Ti–V) = 2.70 Å with energies very close to those of the octets. Although they adiabatically correlate with the ground state atomic asymptote, their origin can be traced to the first excited channel, Ti($^3$F) + V($^6$D), through

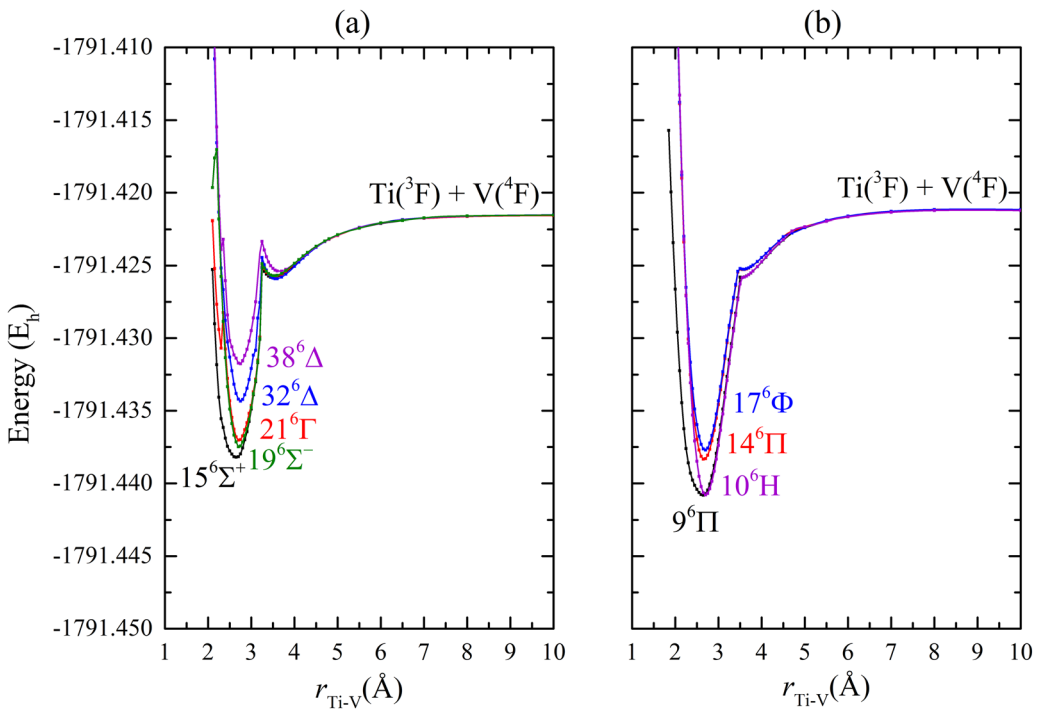


Fig. 4 Potential energy curves of the nine lowest sextet states of TiV at the MRCI/cc-pVQZ level of theory: (a) 15$^6\Sigma^+$, 19$^6\Sigma^-$, 21$^6\Gamma$, 32$^6\Delta$, 38$^6\Delta$ and (b) 9$^6\Pi$, 10$^6$H, 14$^6\Pi$, 17$^6\Pi$.

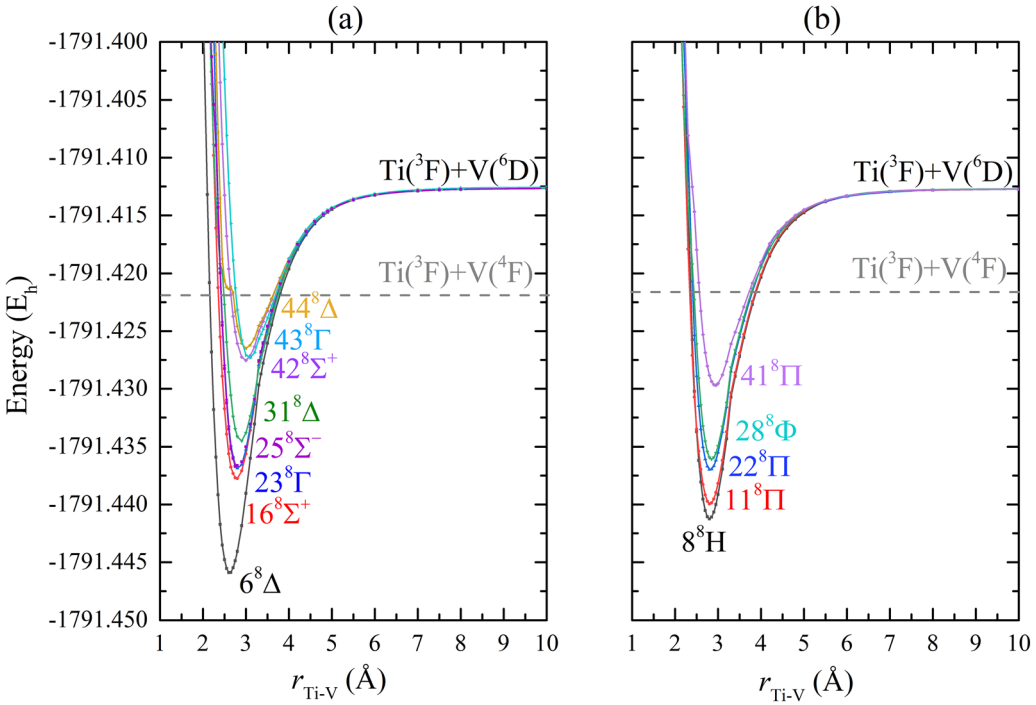


Fig. 5 Potential energy curves of the thirteen lowest octet states of TiV at the MRCI/cc-pVQZ level of theory: (a) $6^8\Delta$, $16^8\Sigma^+$, $23^8\Gamma$, $25^8\Sigma^-$, $31^8\Delta$, $42^8\Sigma^+$, $43^8\Gamma$, $44^8\Delta$ and (b) $8^8H$, $11^8\Pi$, $22^8\Pi$, $28^8\Phi$, $41^8\Pi$.

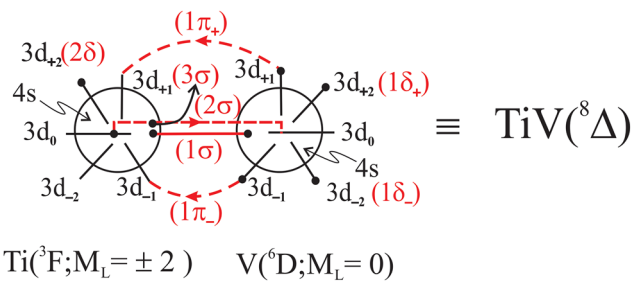


Scheme 4

avoided crossings at $r$(Ti–V) = 3.20-3.50 Å. Their equilibrium MRCI wavefunctions and Mulliken populations support a binding mode consistent with Scheme 4 but with the unpaired electrons coupled into a sextet.

Finally, it should be noted that all secondary minima in the quartet and doublet PECs mentioned before, exhibit exactly the same characteristics; therefore they correspond to the first excited atomic asymptote, as well.

### 3.4 Binding energies of $X^4\Sigma^-$, $1^2\Delta$, and $4^4\Pi$

In the previous discussion of the TiV ground state it was pointed out that the calculated binding energy at the MRCI(+Q)/cc-pVQZ level (Table 1) was significantly lower than the existing experimental value, $D_0^0$ = 2.068 eV = 47.7 kcal mol$^{-1}$.[4] Now, in this section we will examine this discrepancy in detail. To this end, complete basis set (CBS) extrapolation calculations were performed using the cc-pV$n$Z bases, with $n$ = $T$, $Q$, 5 (CBS-TQ5), at the MRCI and MRCI + Q level. Scalar relativistic effects were, also, included *via* the third order Douglas–Kroll–Hess (DKH) correction, MRCI + DKH and MRCI + DKH + Q (Tables 2 and 3).

For the extrapolation, a simple exponential formula was employed, namely

$$E(n) = E(\mathrm{CBS}) + A\exp(-Bn)$$

where $n$ is the basis set cardinal number and $A$, $B$ fitting parameters.

All our results for TiV($X^4\Sigma^-$) are summarized in Table 2. This Table reports absolute energies at equilibrium, as well as those of the asymptotic Ti($^3$F) + V($^4$F) and Ti($^5$F) + V($^6$D) channels. The corresponding energy separations are also given, along with the adiabatic and non-adiabatic binding energies of TiV($X^4\Sigma^-$). We note here that the computation of the Ti($^5$F) + V($^6$D) asymptotic energy was technically feasible using a spin multiplicity of 10 at infinite separation.

In Table 2, we see a gradual increase in binding energy with increasing quality of the basis set and also a small additional improvement from the introduction of scalar relativistic corrections. At the MRCI + DKH + Q/CBS-TQ5 level, the non-adiabatic (intrinsic) binding energy of TiV($X^4\Sigma^-$) is $D_e' = 2.860$ eV and taking into account the energy difference between the two asymptotic channels, $\Delta E_\infty$ = 1.159 eV (Table 2), we obtain $D_e^0$ = 1.701 eV, with respect to the ground state atomic limit Ti($^3$F) + V($^4$F). This yields $D_0^0$ = 1.678 eV using the spectroscopic constants of Table 1. A further correction can result from the small error in the calculation of the energy gap between the Ti($^3$F) + V($^4$F) and Ti($^5$F) + V($^6$D) asymptotes: 1.159 eV (Table 2) compared to the experimental ($M_J$ averaged) 1.051 value.[9]

Table 2 Equilibrium bond lengths $r_e$ (Å) and energies $E$ ($E_h$) of TiV($X^4\Sigma^-$), asymptotic energies $E_\infty$ and $E'_\infty$ ($E_h$) of the atomic channels Ti($^3$F) + V($^4$F) and Ti($^5$F) + V($^6$D), respectively, and corresponding energy separations $\Delta E_\infty$ (eV), adiabatic and non-adiabatic binding energies $D_e$ and $D'_e$ (eV) of TiV($X^4\Sigma^-$) at different levels of theory and with cc-pV$n$Z basis sets, with $n$ = $T$ ($T\zeta$), $Q$ ($Q\zeta$), 5($5\zeta$). Extrapolation to the complete basis set (CBS) limit are also given

| Basis set | $r_e$ | $-E$ | $-E_\infty$ | $-E'_\infty$ | $\Delta E_\infty$ | $D_e$ | $D_e^{'}$ |
|---|---|---|---|---|---|---|---|
| **MRCI** | | | | | | | |
| T$\zeta$ | 1.921 | 1791.45399 | 1791.41832 | 1791.36829 | 1.361 | 0.971 | 2.332 |
| Q$\zeta$ | 1.899 | 1791.47043 | 1791.42060 | 1791.37935 | 1.123 | 1.356 | 2.479 |
| 5$\zeta$ | 1.894 | 1791.47585 | 1791.42527 | 1791.37996 | 1.233 | 1.377 | 2.610 |
| CBS | | 1791.47852 | 1791.42790 | 1791.37999 | 1.304 | 1.378 | 2.681 |
| **MRCI + Q** | | | | | | | |
| T$\zeta$ | 1.928 | 1791.4618 | 1791.4211 | 1791.3732 | 1.301 | 1.110 | 2.411 |
| Q$\zeta$ | 1.907 | 1791.4793 | 1791.4292 | 1791.3849 | 1.205 | 1.365 | 2.569 |
| 5$\zeta$ | 1.902 | 1791.4851 | 1791.4320 | 1791.3858 | 1.258 | 1.444 | 2.701 |
| CBS | | 1791.4879 | 1791.4335 | 1791.3859 | 1.297 | 1.478 | 2.775 |
| **MRCI + DKH** | | | | | | | |
| T$\zeta$ | 1.929 | 1801.06546 | 1801.02110 | 1800.97344 | 1.297 | 1.152 | 2.449 |
| Q$\zeta$ | 1.908 | 1801.08044 | 1801.03325 | 1800.98326 | 1.360 | 1.284 | 2.644 |
| 5$\zeta$ | 1.904 | 1801.08632 | 1801.03424 | 1800.98618 | 1.308 | 1.415 | 2.725 |
| CBS | | 1801.08944 | 1801.03424 | 1800.98742 | 1.274 | 1.502 | 2.776 |
| **MRCI + DKH + Q** | | | | | | | |
| T$\zeta$ | 1.936 | 1801.0714 | 1801.0230 | 1800.9789 | 1.200 | 1.319 | 2.519 |
| Q$\zeta$ | 1.916 | 1801.0894 | 1801.0356 | 1800.9894 | 1.256 | 1.466 | 2.722 |
| 5$\zeta$ | 1.912 | 1801.0957 | 1801.0364 | 1800.9926 | 1.193 | 1.613 | 2.806 |
| CBS | | 1801.0990 | 1801.0365 | 1800.9939 | 1.159 | 1.701 | 2.860 |

Table 3 Equilibrium bond lengths $r_e$ (Å) and energies $E$ ($E_h$), adiabatic and non-adiabatic binding energies $D_e$ and $D'_e$ (eV) (with respect to Ti($^3$F) + V($^4$F) and Ti($^5$F) + V($^6$D), respectively) and energy separations $T_e$ (cm$^{-1}$) of TiV($1^2\Delta$ and $4^4\Pi$) at different levels of theory and with cc-pV$n$Z basis sets, with $n$ = $T$ ($T\zeta$), $Q$ ($Q\zeta$), 5 ($5\zeta$). Extrapolation to the complete basis set (CBS) limit are also given

| | $1^2\Delta$ | | | | | $4^4\Pi$ | | | | |
|---|---|---|---|---|---|---|---|---|---|---|
| Basis set | $r_e$ | $-E$ | $D_e$ | $D_e^{'}$ | $T_e$ | $r_e$ | $-E$ | $D_e$ | $D_e^{'}$ | $T_e$ |
| **MRCI** | | | | | | | | | | |
| T$\zeta$ | 1.942 | 1791.44837 | 0.818 | 2.179 | 1233 | 2.029 | 1791.43790 | 0.533 | 1.894 | 3531 |
| Q$\zeta$ | 1.925 | 1791.46440 | 1.192 | 2.314 | 1324 | 2.009 | 1791.45280 | 0.876 | 1.999 | 3869 |
| 5$\zeta$ | 1.923 | 1791.47022 | 1.223 | 2.456 | 1237 | 2.005 | 1791.45799 | 0.890 | 2.123 | 3921 |
| CBS | | 1791.47353 | 1.242 | 2.545 | 1095 | | 1791.46076 | 0.894 | 2.198 | 3902 |
| **MRCI + Q** | | | | | | | | | | |
| T$\zeta$ | 1.946 | 1791.4563 | 0.978 | 2.259 | 1207 | 2.042 | 1791.4466 | 0.695 | 1.996 | 3336 |
| Q$\zeta$ | 1.931 | 1791.4732 | 1.199 | 2.404 | 1339 | 2.023 | 1791.4625 | 0.906 | 2.111 | 3687 |
| 5$\zeta$ | 1.927 | 1791.4794 | 1.290 | 2.547 | 1251 | 2.018 | 1791.4680 | 0.980 | 2.237 | 3753 |
| CBS | | 1791.4803 | 1.273 | 2.570 | 1668 | | 1791.4710 | 1.019 | 2.316 | 3709 |
| **MRCI + DKH** | | | | | | | | | | |
| T$\zeta$ | 1.943 | 1801.05872 | 1.024 | 2.321 | 1478 | 2.030 | 1801.04791 | 0.729 | 2.649 | 3851 |
| Q$\zeta$ | 1.929 | 1801.07565 | 1.154 | 2.514 | 1051 | 2.011 | 1801.06356 | 0.825 | 2.185 | 3705 |
| 5$\zeta$ | 1.927 | 1801.08175 | 1.293 | 2.601 | 1003 | 2.007 | 1801.06908 | 0.948 | 2.256 | 3784 |
| CBS | | 1801.08519 | 1.386 | 2.661 | 933 | | 1801.07209 | 1.030 | 2.304 | 3808 |
| **MRCI + DKH + Q** | | | | | | | | | | |
| T$\zeta$ | 1.949 | 1801.0667 | 1.190 | 2.390 | 1032 | 2.043 | 1801.0568 | 0.920 | 2.119 | 3204 |
| Q$\zeta$ | 1.935 | 1801.0846 | 1.334 | 2.590 | 1054 | 2.024 | 1801.0734 | 1.030 | 2.286 | 3512 |
| 5$\zeta$ | 1.932 | 1801.0910 | 1.487 | 2.680 | 1032 | 2.020 | 1801.0793 | 1.166 | 2.360 | 3599 |
| CBS | | 1801.0947 | 1.584 | 2.742 | 944 | | 1801.0825 | 1.252 | 2.411 | 3621 |

This difference of 0.108 eV should be added to $D_0^0$ to arrive at a final value of $D_0^0$ = 1.786 eV = 41.1 kcal mol$^{-1}$. This is our best value for the binding energy of TiV($X^4\Sigma^-$) but it is still lower by 0.282 eV than the experimental one reported by Spain and Morse[4] using the R2PI technique. Certainly, other subtle factors could influence our results, *e.g.* core correlation effects which, however, do not have such a significant impact on the binding energies. In the present work, it was beyond our computational possibilities to correlate 16 additional core electrons even at the CISD level.

A final remark concerns the fact that our small difference, of 0.282 eV, from the experimental value, closely matches the first excitation energy of V, $\Delta E(^4\text{F} \leftarrow {}^6\text{D})$ = 0.245 eV.[9] If, in the R2PI experiment, the outgoing V atom were produced in its first excited state, $^6$D, the experimentally determined $D_0^0$ value would be larger by this amount, thereby accounting for our computed value. However, this interpretation remains speculative.

In Table 3, we present a similar analysis for the $1^2\Delta$ and $4^4\Pi$ states. Our primary objective was to assess whether the $1^2\Delta$ state remains above the ground state at higher levels of theory and, also, to determine an accurate $\Delta E(X^4\Sigma^- \leftarrow 4^4\Pi)$ excitation energy. From Table 3, at the MRCI + DKH + Q/CBS-TQ5 level, we have $T_e$ values: 944 cm$^{-1}$ ($1^2\Delta$) and 3621 cm$^{-1}$ ($4^4\Pi$). These

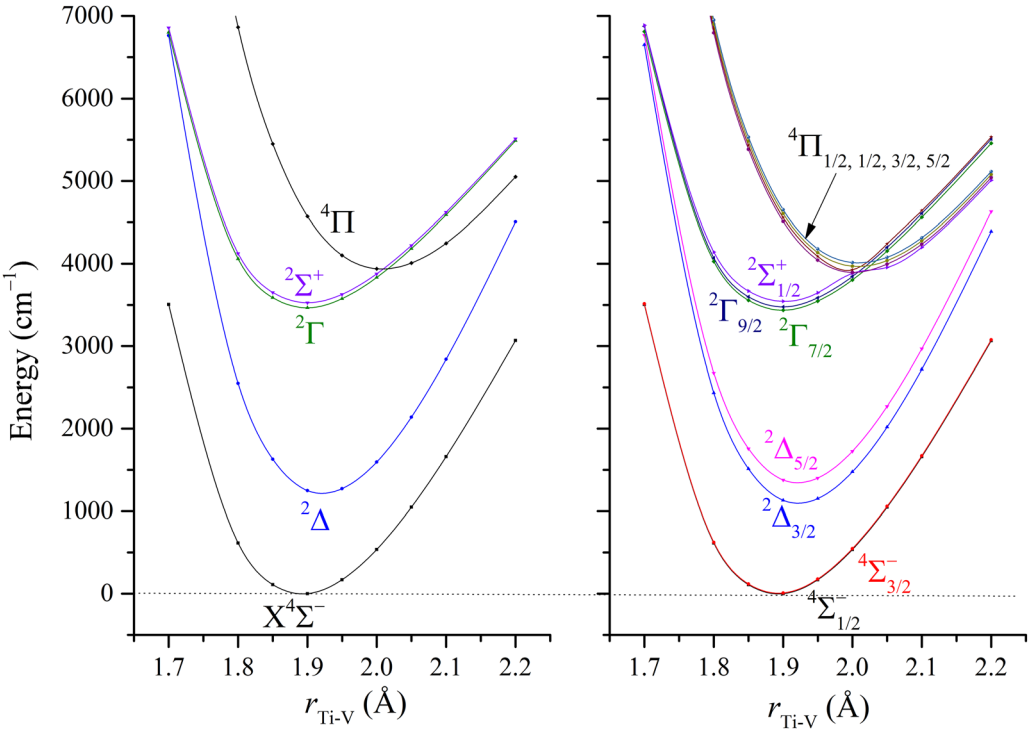


Fig. 6 Potential energy curves of the five lowest-lying Λ–S states of TiV around their equilibrium distances (left) and corresponding Ω states (right) as they were calculated by including spin–orbit coupling at the MRCI/cc-pVQZ level of theory.

results are in close agreement with the corresponding results of Table 1.

The binding energies, $D_e$, of both states increase by, roughly, the same amount as that of the ground state at the MRCI + DKH + Q/CBS-TQ5 level. We recall here that both states $1^2\Delta$ and $4^4\Pi$ originate non-adiabatically from the excited Ti($^5$F) + V($^6$D) asymptote, like the ground TiV($X^4\Sigma^-$) state. As a general rule, we could say that these observations apply to all states intrinsically correlating with the same dissociation channel.

Concluding this section, we found it interesting to examine the effect of spin–orbit coupling (SOC) on some of the lowest-lying states of TiV. To this end, the five lowest Λ–S states were used to diagonalize the Breit–Pauli operator in the region around their equilibrium distances at the MRCI/cc-pVQZ level. Our results are summarized in Fig. 6. As shown, SOC splittings are generally very small, and cannot in any way quantitatively alter the above results. For example, the $^2\Delta_{3/2}$–$^2\Delta_{5/2}$ splitting is approximately 250 cm$^{-1}$, while for the ground state, which is a Σ state, the splitting is only 10 cm$^{-1}$. The overall picture remains largely unchanged, except for a few avoided crossings between some higher states with $\Omega$ = 1/2 near r(Ti–V) = 2.00 Å. These findings indicate that inclusion of SOC does not significantly alter our potential energy curve profiles. The TiV molecule is primarily described by Hund's case (a); however, SOC can induce couplings between energetically close-lying states, thereby subtly modifying the qualitative picture and accounting for some weak features in the TiV spectrum. A treatment of all 45 states, including SOC effects, would constitute a separate future study.

## 4. Summary and conclusions

We have employed the multireference complete active space MRCISD methodology in conjunction with high quality correlation consistent basis sets to study 45 low-lying Λ–S electronic states of the TiV diatomic system.

For the first time full potential energy curves were constructed for all states considered, and corresponding spectroscopic constants were extracted.

The ground state was unambiguously found to be of $X^4\Sigma^-$ symmetry, in agreement with the experimental observations.[1] Its potential energy curve adiabatically correlates with the ground state atomic asymptote, Ti($^3$F) + V($^4$F). However, its morphology is modulated by successive avoided crossings with curves originating from higher atomic channels, namely Ti($^3$F) + V($^6$D) and Ti($^5$F) + V($^6$D). As a result it exhibits a double-well shape with an additional shallow vdW minimum at long distance. The global minimum corresponding to TiV($X^4\Sigma^-$) is located at $r_e$ = 1.910 Å, while our best value for its adiabatic binding energy was found $D_0^0$ = 1.786 eV = 41.1 kcal mol$^{-1}$, relative to the ground state Ti($^3$F) + V($^4$F) atomic limit, in reasonable agreement with the corresponding experimental value.[4] We note that, since $X^4\Sigma^-$ stems from the Ti($^5$F) + V($^6$D) asymptote, its intrinsic bond strength can be evaluated as $D_0$ = 1.786 eV + 1.051 eV = 2.837 eV = 65.4 kcal mol$^{-1}$; a rather large value.

Several other states, doublets and quartets, exhibit the same double-well feature. A similar rationale applies in these cases.

All sextet and octet states considered in the present work, trace their lineage to the first excited atomic asymptote Ti($^3$F) + V($^6$D) and have relatively small binding energies.

The first excited state of TiV is $1^2\Delta$, lying only 944 $cm^{-1}$ above the $X^4\Sigma^-$ ground state, with $r_e$ = 1.930 Å, and exhibiting a similar electronic structure, reminiscent of its origin in the Ti($^5$F) + V($^6$D) atomic configuration.

Finally, we mention the $4^4\Pi$ state which is located approximately 3500–4000 $cm^{-1}$ higher than $X^4\Sigma^-$, with $r_e$ = 2.020 Å, and could be of interest in a spectroscopic study of TiV. It has a double-well potential energy profile, similar to that of the ground state.

We conclude this paper with the hope that our results will be helpful in a future investigation of the experimentally poorly explored TiV system.

## Author contributions

Magdalene Liosi: writing – original draft, visualization, investigation, formal analysis, data curation. Aristotle Papakondylis: writing – review & editing, writing – original draft, supervision, conceptualization.

## Conflicts of interest

There are no conflicts of interest to declare.

## Data availability

The coordinates of all potential energy curves presented, are provided in the supplementary information (SI). Supplementary information is available. See DOI: https://doi.org/10.1039/d6cp00590j.

## References

1 R. J. Van Zee and W. Weltner Jr, *Chem. Phys. Lett.*, 1984, **107**, 173–177.
2 A. R. Miedema, *Faraday Symp. Chem. Soc.*, 1980, **14**, 136–148.
3 S. P. Walch and C. W. Bauschlicher Jr., in *Comparison of Ab Initio Quantum Chemistry with Experiment for Small Molecules*, ed. R. J. Bartlett, 1985, pp. 17–51, ISBN-13: 978-9401089173.
4 E. M. Spain and M. D. Morse, *J. Phys. Chem.*, 1992, 96, 2479–2486.
5 S. M. Mattar and W. D. Hamilton, *J. Phys. Chem.*, 1992, **96**, 1606–1610.
6 G. L. Gutsev, M. D. Mochena, P. Jena, C. W. Bauschlicher Jr and H. Partridge III, *J. Chem. Phys.*, 2004, **121**, 6785–6797.
7 Y. Jiang and Y.-R. Liu, *J. Chem. Theory Comput.*, 2023, **19**, 8998–9007.
8 M. Liosi and A. Papakondylis, *Chem. Phys. Lett.*, 2025, **867**, 141977.
9 A. Kramida, Y. Ralchenko and J. Reader, NIST ASD Team, NIST Atomic Spectra Database (ver. 5.11) available https://physics.nist.gov/asd (2024, October 31).
10 N. B. Balabanov and K. A. Peterson, *J. Chem. Phys.*, 2005, **123**, 064107–064115.
11 M. Douglas and N. M. Kroll, *Ann. Phys.*, 1974, **82**, 89.
12 B. A. Hess, *Phys. Rev. A*, 1986, **33**, 3742.
13 H.-J. Werner and P. J. Knowles, *J. Chem. Phys.*, 1988, **89**, 5803–5814.
14 M. M. F. de Moraes and Y. A. Aoto, *J. Phys. Chem. A*, 2023, **127**, 10075–10090 and references therein.
15 E. R. Davidson and D. W. Silver, *Chem. Phys. Lett.*, 1977, **52**, 403.
16 H.-J. Werner and P. J. Knowles, *et al.*, *WIREs Comput. Mol. Sci.*, 2012, **2**, 242–253.
17 H.-J. Werner and P. J. Knowles, *et al.*, *J. Chem. Phys.*, 2020, **152**, 144107.

 